




# Microstructure–properties relationship in ethylene-propylene diene monomer (EPDM)/nitrile butadiene rubber (NBR)/halloysite nanotubes (HNTs) nanocomposites

Seyed Mohamad Reza Paran<sup>1</sup> · Ghasem Naderi<sup>1</sup> · Moslem Mirzaee<sup>1</sup> · Mir Hamid Reza Ghoreishy<sup>1</sup> · Marcin Włoch<sup>2</sup> · Amin Esmaeili<sup>3</sup> · Otman Abida<sup>4</sup> · Mohammad Reza Saeb<sup>2</sup> 

Received: 17 April 2022 / Revised: 4 February 2023 / Accepted: 6 February 2023 /  
Published online: 2 March 2023  
© The Author(s) 2023

## Abstract

Structure–properties relationship in complex rubber nanocomposites is a key for enlarging the performance window. Herein, halloysite nanotubes (HNTs) are added at variable content to ethylene-propylene diene monomer (EPDM)/nitrile butadiene rubber (NBR) rubber blends compatibilized with maleic anhydride grafted HNTs to evaluate cure characteristics, along with microstructure, and mechanical and swelling behavior. The crosslinking rate increased by HNTs loading, but the scorch time decreased. Moreover, a 45% rise in tensile strength was observed for systems containing 10 wt% HNTs. SEM and TEM micrographs revealed a rough fracture surface with proper dispersion of HNT within EPDM/NBR. The modulus of EPDM/NBR/HNTs nanocomposites is theoretically estimated by modified Kolarik model, demonstrating a good agreement with experimental value. Dynamic mechanical thermal analysis (DMTA) revealed a higher storage modulus up to 2.27 GPa with the introduction of HNTs into EPDM/NBR compound. Correspondingly, lower solvent uptake (decreased by 38%) is reported. Thermogravimetric analysis (TGA) revealed higher thermal stability for highly-loaded systems.

**Keywords** EPDM · NBR · HNTs · Cure behavior · Mechanical properties · Stiffness · Rubber nanocomposites

✉ Seyed Mohamad Reza Paran  
m.paran@ippi.ac.ir

✉ Mohammad Reza Saeb  
mrsaeb2008@gmail.com

Extended author information available on the last page of the article

## Introduction

Blending rubbers with complementary characteristics to each other enables one to manufacture elastomers with higher performance for advanced applications. The main difficulty, however, is the immiscibility of elastomers on a molecular level or the weak interface between phases not being co-cured. Addition of compatibilizer is well-known as the most practical way to compensate for inadequate interfacial adhesion in elastomer blends. However, it seems unlikely to attain co-crosslinking of elastomers in the presence of reactive nanofillers [1]. Ethylene-propylene diene monomer (EPDM) is an amorphous rubber widely used ranging from automotive and construction to the electronic industries, but it suffers from poor mechanical and oil resistance—necessitating the use of reinforcing agents or complementary polymers [2]. Nitrile butadiene rubber (NBR) has descent hot oil and ozone resistance [3], low-temperature flexibility [4] and appropriate mechanical properties [5]. NBR deserves credit for the ability to co-curing with EPDM, but unavoidably suppresses the stiffness of EPDM [6]. Thus, nanocomposites based on EPDM/NBR have received more attention in both academia and industry.

EPDM/NBR blends reinforced with various types of nanofillers have been the subject of several investigations in order to uncover microstructure–properties interrelationships [7]. Ghassemieh [8] reported the effect of nanoclay on the mechanical properties of EPDM/NBR blends. The incorporation of nanoclay into rubber blends increased the compression resistance of EPDM/NBR blend. Ersali et al. [9] reported the effect of two types of organoclays (Cloisite 20A and Cloisite 30B) on the properties of EPDM/NBR blend and found that the higher mechanical properties could be achieved by the combined use of organoclays. Jovanovic et al. [10] reported that incorporation of nanosilica into EPDM/NBR elastomer blends leads to formation of a nanocomposite with high physical and mechanical properties through interfacial interaction modification. In a recent work [11], we examined combination of graphene and graphene oxide nanoplatelets in EPDM/NBR blends, where dynamic mechanical and dielectric properties significantly improved. Nevertheless, the need for application of low-cost and highly reactive nanofillers has directed our attention toward nanofillers from clay family other than carbonaceous nanofillers.

Halloysite nanotubes (HNTs) are superior one-dimensional nanominerals with predominantly hollow tubular nanostructure and very high aspect ratio. Due to their relatively high mechanical and thermal stability, along with biocompatibility, HNTs are good candidates to be added to polymeric matrices [12]. They are also economically reasonable enough to be considered as alternatives for multi-walled carbon nanotubes (MWCNTs) [13]. In this sense, various polymer/HNTs nanocomposites have been prepared via melt compounding [14]. On the basis of open literature, HNTs have been used in manufacturing numerous thermoplastic and thermoset polymer systems such as polypropylene [15], polyamides [16], polyethylene [17], natural rubber [18], EPDM [19] and epoxy resins [20] for thermal, physical and mechanical properties enhancement. In some cases, the properties

of nanocomposites containing pristine HNTs and organoclay were compared and discussed, demonstrating the edge of HNTs in view of its higher stiffness and aspect ratio over the nanoclay [21]. However, to the best of our knowledge, there is no report on the effect of HNTs on the microstructure and properties of EPDM/NBR blends.

In light of above discussions, the objective of the current work was to study the effect of HNTs incorporation and loading level on the cure characteristics, morphology, mechanical properties and thermal properties of EPDM/NBR blends in the presence of a proper content of a compatibilizer, namely maleated EPDM (MAH-g-EPDM). Since HNTs are reactive toward curing, because of hydroxyl functional groups, the pristine HNTs was added to the compatibilized EPDM/NBR elastomer blends and the aforementioned characteristics of the resulting nanocomposites were compared to the unreinforced rubber blend. Then, it was attempted to correlate the microstructure and curing characteristics with the thermal and mechanical properties of EPDM/NBR elastomer nanocomposites. The amount of HNTs was taken as a parameter in this investigation. In addition, the modified version of cross-orthogonal skeleton model (COS) conceptual model originally proposed by Kolarik was used in order to impart deeper understanding of the effects of nanotubes on the mechanical behavior of the complex nanocomposites based on EPDM/NBR/HNTs.

## Theoretical background

The Young's moduli of the compatibilized EPDM/NBR nanocomposites were evaluated on the basis of Kolarik equation, which was suggested to predict the modulus of particulate polymer composites by considering three perpendicular plates (3PP) model [22]:

$$E_c = E_m f(2 - f) + \frac{(1 - f)^2}{\frac{f}{E_m} + \frac{1 - f}{E_f}} \quad (1)$$

where  $f$  is related to the volume fraction of filler through the following equation [22]:

$$f = 1 - \varphi_f^{\frac{1}{3}} \quad (2)$$

Moreover,  $E_m$  and  $E_f$  are the Young's moduli of the matrix and filler, respectively.

Since the modulus of HNTs is significantly higher than that of the modulus of the polymer matrix ( $E_f > E_m$ ), the term  $(1 - f)/E_f$  could be neglected in Eq. (1). Therefore, the predicted Young's modulus of nanocomposite could be represented as:

$$E_c = E_m f(2 - f) + E_m \frac{(1 - f)^2}{f} \quad (3)$$

The relative modulus ( $E_R = E_c/E_m$ ) of nanocomposites could be calculated from the following equation:

$$E_R = f(2 - f) + \frac{(1 - f)^2}{f} \quad (4)$$

We can use cross-orthogonal skeleton model (COS) to predict the Young's modulus of polymer nanocomposites above the percolation threshold. It is assumed that the network of HNTs formed a continuous phase in EPDM/NBR matrix. The initial form of this model was proposed by Kolarik as the following equation [23]:

$$E_c = E_m(1 - f^2) + E_f f^2 + \frac{2f(1 - f)E_m}{1 - f + f \frac{E_m}{E_f}} \quad (5)$$

$$1 - \varphi_f - (1 - f)^2(1 + 2f) = 0 \quad (6)$$

The simplified model was proposed by Zare on the basis of the above equation [24]:

$$E_R = 1 + \frac{E_f \varphi_f^{1.4}}{E_m} + 2\varphi_f^{0.7} \quad (7)$$

A combination of Eqs. (4) and (7) could be applied to predict the Young's modulus of EPDM/NBR nanocomposites containing both dispersed and networked HNTs [24]:

$$E_R = f(2 - f) + \frac{(1 - f)^2}{f} + \frac{E_N \varphi_N^{1.4}}{E_m} + 2\varphi_N^{0.7} \quad (8)$$

where

$$f = 1 - \varphi_d^{\frac{1}{3}} \quad (9)$$

The volume fractions of networked and dispersed HNTs in Eq. (8) are represented as  $\varphi_N$  and  $\varphi_d$ , respectively. The parameter  $E_N$  is related to the modulus of the networked HNTs.

## Materials and methods

### Materials

Ethylene-propylene diene monomer (EPDM), KEP-270, containing 57 wt% ethylene monomer with viscosity of 71 (ML (1 + 4), 100 °C) was supplied by the Kumho Petrochemical Co. (Korea). Nitrile butadiene rubber (NBR), KNB 35L, containing 33% acrylonitrile with viscosity of 60 (ML (1 + 4), 100 °C) was purchased from Kumho Petrochemical Co. (Korea). Halloysite nanotubes (HNTs), ultrafine grade, with an internal diameter of 15–20 nm and an external diameter of 50–60 nm (claimed by provider), were obtained from Imerys Tableware Asia Limited (New Zealand).

Maleated EPDM (MAH-*g*-EPDM) was prepared in the laboratory [4] using maleic anhydride obtained from Sigma-Aldrich, USA, with 99% of purity. The curing of rubber nanocomposites was carried out by using *N*-cyclohexyl-2-benzothiazole sulfonamide (CBS) and sulfur (S) purchased from Bayer (M) Ltd. (Germany). Other ingredients such as zinc oxide (ZnO) and Stearic acid (St. Ac.) as accelerator and activators were similarly obtained from Bayer (M) Ltd. (Germany) and used without further treatment.

### Nanocomposite preparation

EPDM/NBR/HNTs nanocomposites with various formulations, in accordance with Table 1, were prepared on a laboratory open two-roll mill mixer, running at rotor speed ratio of 1:1.2 for 13 min at 40 °C. In the first stage, EPDM was masticated by two-roll mixing mill for 2 min, then MAH-*g*-EPDM and NBR were sequentially added to the EPDM and mixing was continued for additional 3 min. HNTs was incorporated into the rubber compound, and the mixing was continued for 5 min. Finally, the curing ingredients were added to the rubber nanocomposite and mixed for 3 min. The EPDM/NBR weight ratio was fixed at 70/30 (w/w) for all the prepared samples. The EPDM/NBR compound compatibilized with MAH-*g*-EPDM was also prepared on two-roll mill mixer for 13 min at 40 °C to be used as a reference sample. The prepared rubber compounds were compression molded in a compression molding machine at 160 °C and time needed to reach the required optimum cure was estimated according to the optimum cure time obtained from Monsanto Rheometer.

### Characterization

The cure characteristics of the reference sample and EPDM/NBR nanocomposites containing various amounts of HNTs (all compatibilized with MAH-*g*-EPDM) were studied by using a Monsanto Rheometer R-100 testing instrument operated at 160 °C with 3° arc at a period of 15 min in accordance with ASTM D2084.

**Table 1** Formulations of various EPDM/NBR/HNTs nanocomposites together with the reference sample (compatibilized EPDM/NBR blend) prepared in this work

Sample code	EPDM/ NBR (phr)	MAH- <i>g</i> - EPDM (phr)	HNT (phr)	ZnO (phr)	St. acid (phr)	CBS (phr)	Sulfur (phr)
E70N30	100	2	0	5	2	1.5	2
E70N30H1	100	2	1	5	2	1.5	2
E70N30H3	100	2	3	5	2	1.5	2
E70N30H5	100	2	5	5	2	1.5	2
E70N30H7	100	2	7	5	2	1.5	2
E70N30H10	100	2	10	5	2	1.5	2

The morphology of the compatibilized EPDM/NBR/HNTs nanocomposites was imaged on a Vega II XMU scanning electron microscope (SEM), Czech Republic at magnification of 1000 $\times$ . The samples were cryogenically fractured and coated with gold powders by sputtering technique prior to SEM observations. The nanostructure of the cryogenically microtomed (with a diamond knife at  $-100\text{ }^{\circ}\text{C}$ ) fracture surface of the samples containing HNTs was observed on a Philips CM-200 transmission electron microscope (TEM), the Netherlands, with an accelerating voltage of 100 kV and magnification of 200 kx.

Tensile tests were done according to the ASTM D412 by a Universal tensile testing machine, Instron 6025 model operated at room temperature at an extension speed of 500 mm/min with an initial gage length of 25 mm.

The hardness of the prepared rubber nanocomposites was measured, as per ASTM D2240 testing method by using a Durometer Hardness Tester, TA instruments (USA). The sheets with effective thickness of 6 mm were used for hardness measurements.

The oscillatory response of the EPDM/NBR/HNTs nanocomposites to shear was monitored by dynamic mechanical thermal analysis (DMTA) conducted on a Triton Technology Tritec 2000DMA (UK). The storage modulus and damping factor of the prepared nanocomposites were measured in bending mode at a constant heating rate of  $5\text{ }^{\circ}\text{C}/\text{min}$  and a frequency of 1 Hz in a strain of 0.02 mm from  $-100$  to  $100\text{ }^{\circ}\text{C}$ .

Swelling behavior/capacity of the various EPDM/NBR/HNTs nanocomposites was investigated in toluene solvent in accordance with ASTM D5964. The required samples were cut from the molded slabs and weighted in dry state. The swollen weights of each nanocomposite immersed in solvent for 72 h were recorded to determine the swelling ratio and the crosslink density obtained using Flory–Rehner equation [25]:

$$Q_s = \frac{w_s - w_u}{w_u} \quad (10)$$

$$v_{sw} = \frac{-[\ln(1 - v) + v + \chi v^2]}{V_s \left( v^{\frac{1}{3}} - \frac{v}{2} \right)} \quad (11)$$

where  $Q_s$  is the swelling ratio, and  $w_s$  and  $w_u$  are the swollen and unswollen weights of the samples, respectively. The parameter,  $v_{sw}$ , is the crosslink density ( $\text{mol}/\text{m}^3$ ),  $\chi$  is the polymer–solvent interaction parameter,  $V_s$  is the molar volume of the solvent ( $\text{m}^3/\text{mol}$ ) and  $v$  is the volume fraction of polymer in swollen state, which could be calculated from the following equation [25]:

$$v = \frac{\frac{w_p}{d_p}}{\frac{w_p}{d_p} + \frac{w_s}{d_s}} \quad (12)$$

where  $w_p$  and  $w_s$  are the weight fractions of the rubber and solvent in the swollen sample, respectively. The parameters  $d_p$  and  $d_s$  are defined as the densities of

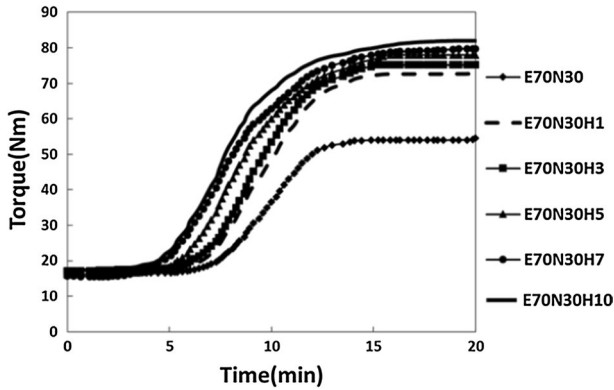


**Fig. 1** Cure curves of the EPDM/NBR nanocomposites containing various loadings of HNTs together with the reference sample (compatibilized EPDM/NBR blend)

**Table 2** Cure characteristics of the compatibilized EPDM/NBR/HNTs nanocomposites together with the reference sample (compatibilized EPDM/NBR blend)

Sample code	t5(min)	t10(min)	t90(min)	t95(min)	$M_H$ (Nm)	$M_L$ (Nm)	$M_H - M_L$ (Nm)
E70N30	7.01	7.58	15.00	17.34	54.5	13.07	41.43
E70N30H1	6.70	7.24	14.25	16.90	72.9	15.65	55.94
E70N30H3	6.62	7.04	14.10	16.76	75.30	15.94	59.35
E70N30H5	6.35	6.85	13.90	16.61	78.00	16.50	61.50
E70N30H7	5.90	6.24	13.50	16.41	79.80	17.73	62.07
E70N30H10	5.68	6.03	13.10	15.76	82.00	18.55	63.54

polymer and solvent, respectively. The polymer–solvent interaction parameter was calculated using the following equation [25]:

$$\chi = 0.487 + 0.228v \tag{13}$$

Thermogravimetric analysis (TGA) was conducted on a Netzsch TG 209 apparatus. Samples were placed in a corundum dish and measurements were conducted in nitrogen atmosphere in the temperature range 25–700 °C at a heating rate of 10 °C/min.

## Results and discussion

### Cure characteristics

The cure behavior of the EPDM/NBR blends containing various loadings of HNTs is shown in Fig. 1. The relevant cure parameters of the nanocomposites are extracted from the figure and summarized in Table 2. Overall, the curves of nanocomposites are all well above that of the reference EPDM/NBR blend compatibilized with

MAH-*g*-EPDM reactive precursor, evidence for the interfacial interaction modification by the introduction of HNTs. This suggests that the addition of HNTs could assist in interfacial adhesion improvement, because of the reactive nature of this nanotube [26]. Moreover, samples containing higher amounts of HNTs have lower scorch time and similarly cure time with respect to the reference compatibilized EPDM/NBR blend. On the other hand, according to Table 2, the maximum torque value and the torque difference were both increased with the HNTs loading, which can be attributed to the effect of nanotubes on the extent of crosslinking and reinforcing effect toward elastomer blend [27].

### Morphological observations

Morphology of such a complicated system could unravel the texture/topography of the fracture surface exhibiting the uniformity and roughness of the surface (SEM micrographs support this evaluation) as well as the presence and dispersion/distribution fashion of nano-scale fillers and polymer domains (TEM images support this evaluation). Figure 2 shows SEM micrographs taken from tensile fracture surface of the reference blend (MAH-*g*-EPDM compatibilized EPDM/NBR) and nanocomposite containing 5 wt% HNTs. The introduction of HNTs into rubber blend resulted in a more irregular texture at the fracture surface, which is characteristic of enhanced interfacial bonding between the rubber matrix and the nanofiller. Parallel lines formed on the fracture surface reveal the direction of fracture propagation, which can be taken as another evidence resulting from the presence of longitudinal nanotubes that resisted against rupture. Guo et al. [27] reported an almost similar morphology in the case of styrene-butadiene rubber matrix reinforced with HNTs, and highlighted the improved interfacial bonding between the polymer matrix and nanofiller aided by the addition of methacrylic acid, which bonds both constituents through grafting/hydrogen bonding mechanism. Application of the mentioned

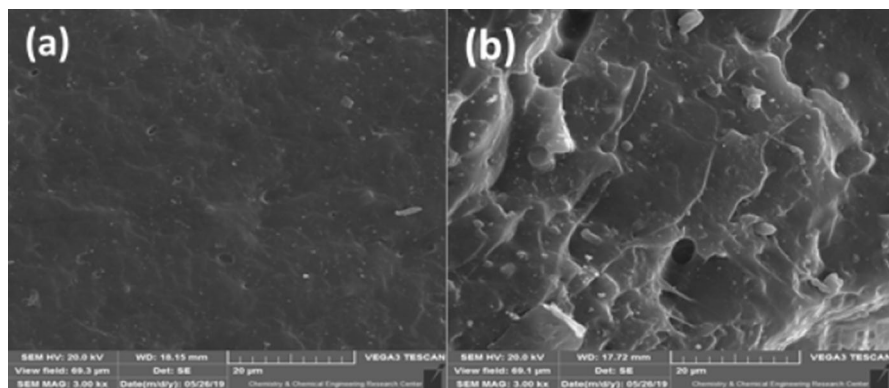


**Fig. 2** SEM photomicrographs of the fracture surfaces taken from tensile testing of the (a) reference (compatibilized EPDM/NBR) blend (E70N30) and (b) EPDM/NBR nanocomposite containing 5 wt% of HNTs (E70N30H5)



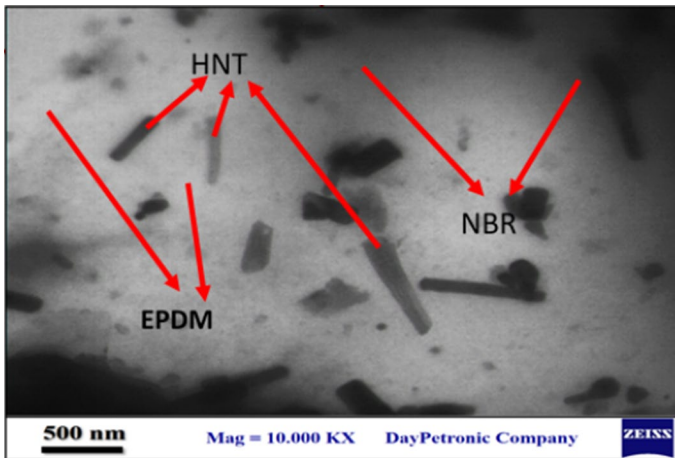


**Fig. 3** TEM photomicrograph of the EPDM/NBR nanocomposites containing 5 wt% of HNTs (E70N30H5). Each component in the blend is graphically distinguished

modifier resulted in a higher mechanical properties, which was additionally proved by intensified roughness of the fracture surface with respect to the neat rubber.

Figure 3 is a closer snapshot of the state of interfacial adhesion and dispersion of domains taken from TEM from the cryogenically microtomed fracture surface of E70N30H5. Bright regions indicate the EPDM phase, while darker ones are representative of NBR phase, distinguished based on different densities of phases. Based on morphological analyses, the length of HNTs varies in between 350 and 790 nm, while its diameter is around 80–100 nm. The used nanofiller is uniformly distributed in the rubber phase, which suggests that the interaction between rubber matrix and nanotubes is higher than that between nanotubes themselves. It also confirms that the appropriate preparation conditions were achieved. A similar state of dispersion was observed by Rooj et al. [18] for natural rubber-based systems with HNTs compatibilized with silane coupling agent. It is also known from the literature that higher loadings of HNTs in rubber composites may lead to the formation of nanofiller aggregates, which reduce the tensile strength of final nanocomposites [28]. In our study, aggregates of HNTs were not observed.

### Mechanical properties

Figure 4 compares the effect of HNTs presence and content on the various parameters related to the mechanical behavior of the reference sample and the nanocomposites. Figure 4a suggests that an average increase in tensile strength up to 45% is the result of addition of HNTs to the EPDM/NBR compound. However, the elongation at break was suppressed slightly with higher amount of nanotubes, as depicted in Fig. 4b, which can be ascribed to some restrictions in chain mobility of polymer matrix induced by the incorporation of nanotubes [29]. Figure 4c shows that the introduction of HNTs into the EPDM/NBR matrix

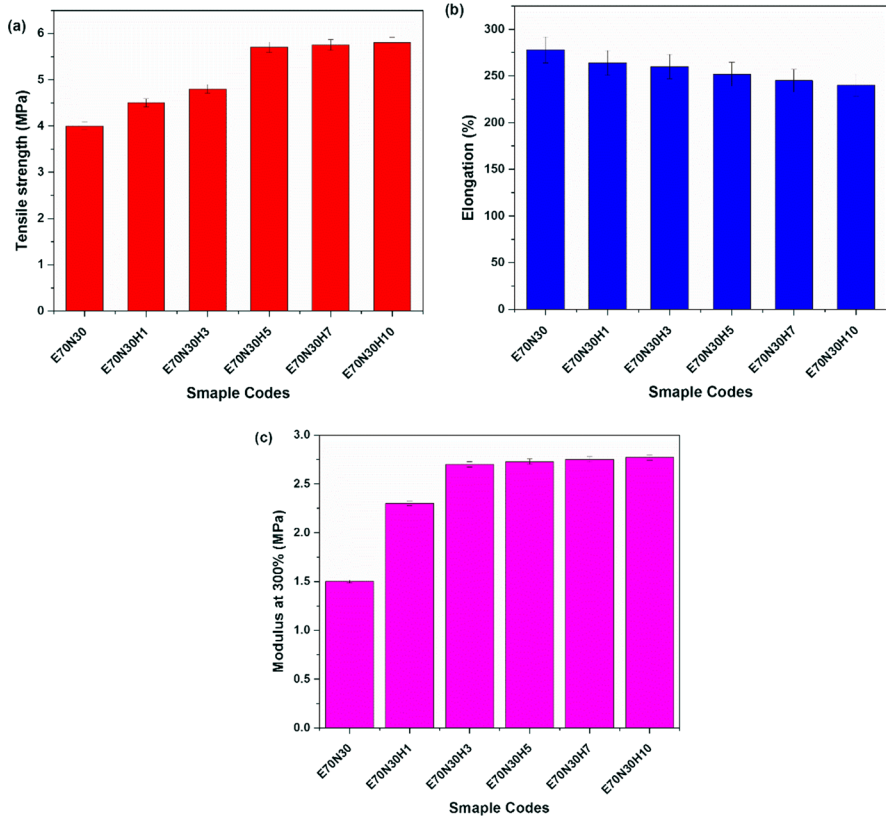


**Fig. 4** Mechanical properties of various EPDM/NBR/HNTs nanocomposites together with the reference sample (compatibilized EPDM/NBR blend); (a) tensile strength, (b) elongation at break, and c modulus at 300% elongation

leads to a higher modulus at 300% elongation, which is attributed to the dispersion state of nanotubes and their interactions with the polymer matrix [30]. The enhanced interaction between the rubber and HNTs was already confirmed by SEM and TEM observations (Figs. 2 and 3). A strong interfacial bonding between the polymer matrix and the applied nanofiller obviously boosted the mechanical properties, due to the effective stress transfer between the polymer matrix and HNTs [31], which is in agreement with theoretical investigations of systems containing nanotubes of different type [32]. Tensile strength and modulus are increased mostly because of higher amounts of HNTs, while elongation at break inversely correlated with HNTs content. Since the amount of MAH-g-EPDM is constant, less compatibilizer could be shared with interfacial zone between rubbers and HNTs, such that elongation at break decreased as a consequence of less interfacial bonding in highly HNTs loaded systems.

## Stiffness analysis

The effect of the amount of HNTs on the modulus of EPDM/NBR nanocomposites was conceptually predicted using Eq. (8). The modulus of EPDM/NBR matrix was estimated from the tensile behavior of the rubber blend at 300% elongation ( $E_m = 1.5$  MPa), while that of the networked HNTs was adopted equal to 30 GPa on the basis of a previous work [33]. The volume percent of HNTs was calculated from the weight percent of each formulation considering the density of HNTs. The volume fractions of the networked and dispersed HNTs were calculated by using optimization toolbar of MATLAB program to minimize the differences between the predicted and experimental moduli of the nanocomposites. The difference between stiffness values of the nanocomposites are compared in Fig. 5. The results supported the effectiveness of loading and dispersion state of HNTs to the modulus of the prepared nanocomposites. A comparison between the theoretical and experimental moduli indicated some deviation at low loading of HNTs, possibly because of the role of interaction underestimated by the theory because of perfect adhesion assumption. At higher loadings, however, the predictions are apparently closer to the experimental values, because of the insensitivity of model to interfacial interaction. In the other word, adhesion parameters are not sensitive to HNTs amount. Therefore, the inaccuracy of the model in prediction of stiffness of such a complex system in which both the compatibilizer and HNTs are present is related to the lack of sense of model to the estimated volume fractions of the networked and dispersed HNTs in EPDM/NBR/MAH-*g*-EPDM/HNTs nanocomposites. Nevertheless, estimations still remain promising for future investigations.

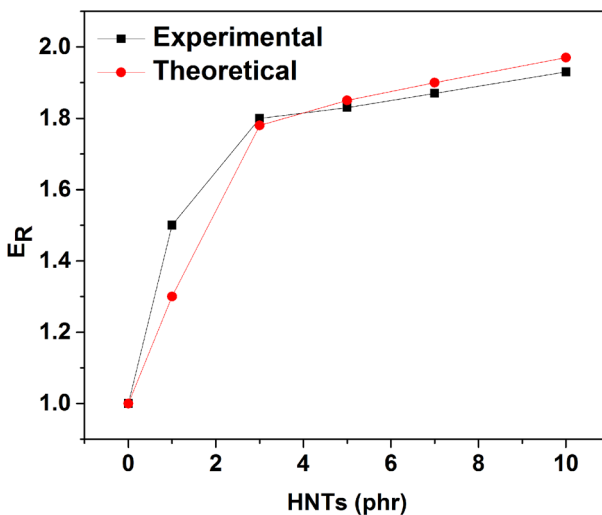


**Fig. 5** Comparison between the theoretical stiffness and experimental values for modulus at 300% elongation of EPDM/NBR nanocomposites as a function of HNTs content

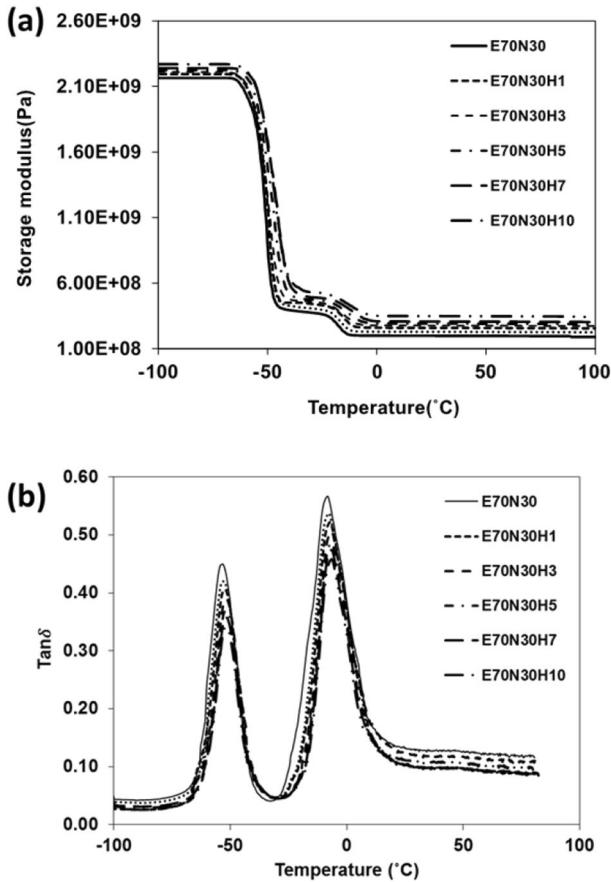


**Fig. 6** The results of DMTA measurements of various EPDM/NBR/HNTs together with the reference sample (compatibilized EPDM/NBR blend)

### DMTA analysis

The results of DMTA measurements conducted on EPDM/NBR/HNTs nanocomposites and the reference blend are compared in Fig. 6. The stiffening effect of HNTs and its interaction with rubber matrix leads to a higher value of storage modulus for compatibilized EPDM/NBR blends, especially those with higher amounts of HNTs, as illustrated in Fig. 6a. Changes in the damping factor ( $\tan \delta$ ) with sweeping temperature in Fig. 6b show reduction with higher HNTs loading in the EPDM/NBR/HNTs nanocomposites. This can be attributed to the restricted mobility of polymer chains induced by the interaction between nanotubes and rubber phases [34]. Furthermore, the behavior of  $\tan \delta$  against temperature in Fig. 6b indicated an increase in glass–rubber transition temperature ( $T_g$ ) of both EPDM and NBR phases, which intensifies the interpretations based on the restricted chain mobility [35].

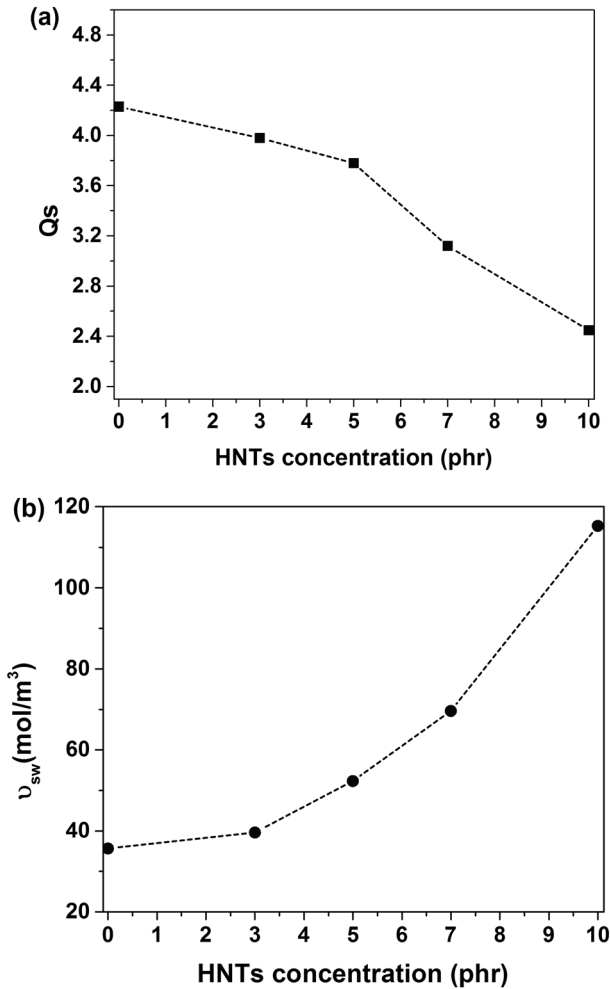


**Fig. 7** Swelling behavior of EPDM/NBR nanocomposites containing various HNTs amounts together with the reference sample (compatibilized EPDM/NBR blend); (a) swelling ratio, and (b) cross-link density. On average, standard deviations after five times repeating the measurements were  $\pm 0.11$  and  $\pm 4.69$  for parts a and b, respectively

### Swelling behavior

The swelling behavior of EPDM/NBR/HNTs nanocomposites is illustrated in Fig. 7. The results indicated a decreased solvent uptake by HNTs loadings up to 38%, which again is assigned to the reinforcement effect of HNTs and the restricted chain extensibility reflected in swelling behavior. The results of the calculated crosslink density are shown in Fig. 7b, indicating a higher value with the HNTs loadings up to 400%, possibly due to the interlocking effect of nanotubes and some physical interactions with the rubber matrix [36].

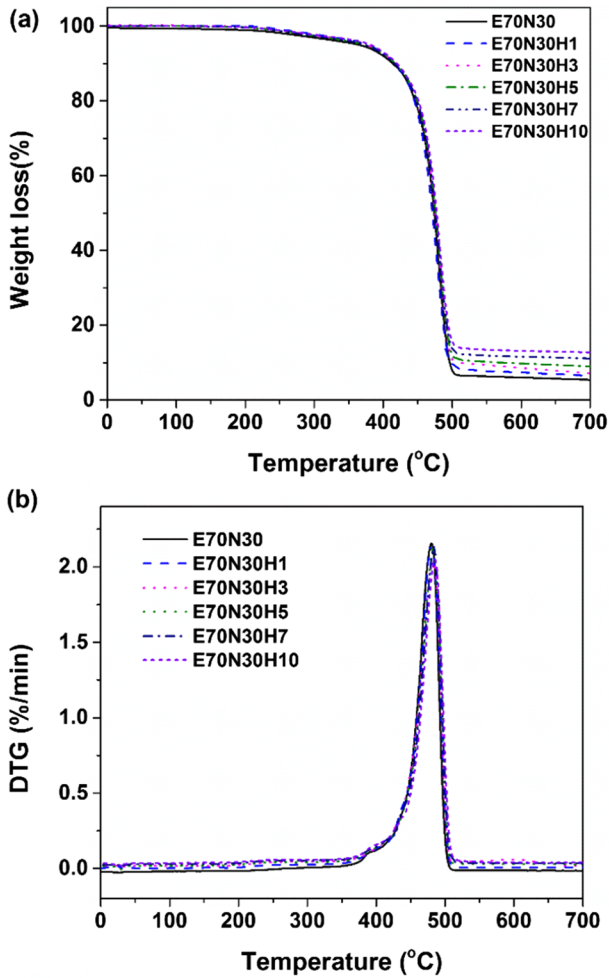


**Fig. 8** The results of TGA and DTG curves of EPDM/NBR/HNTs nanocomposites together with the reference sample (compatibilized EPDM/NBR blend)

## Thermal properties

TGA and derivative TGA (DTG) of EPDM/NBR/HNTs nanocomposites together with those of the reference blend are shown in Fig. 8. It is observed that the introduction of nanotubes into the EPDM/NBR matrix leads to an enhancement of thermal stability of nanocomposites. However, such a thermal stability enhancement did not change the general pathway of thermal degradation at temperatures below 500 °C. A detailed thermal stability evaluation can be carried out by the data extracted from Fig. 8 (Table 3). The results of TGA analysis shown in Table 3 suggest a higher thermal stability in regard with all characteristics. From a molecular view, it may be attributed to the dispersion state of HNTs and its high aspect ratio, which prevents

**Table 3** TGA results for various EPDM/NBR/HNTs nanocomposites together with the reference sample (compatibilized EPDM/NBR blend)

Sample code	Temperature at 5% loss (°C)	Maximum weight loss (%)	Temperature at maximum weight loss rate (°C)
E70N30	368.4	90.43	477.3
E70N30H1	369.9	87.81	479.3
E70N30H3	371.1	87.42	480.7
E70N30H5	371.2	86.65	481.3
E70N30H7	372.1	85.73	482.4
E70N30H10	379.3	83.54	483.1

the emission of small gaseous molecules trapped into the polymer structure at higher temperatures [37].

## Conclusion

Rubber blends based on ethylene-propylene rubber (EPDM) and nitrile butadiene rubber (NBR) are compatibilized with MAH-*g*-EPDM and further reinforced with varying amounts of HNTs on a two-roll mill mixer to prepare nanocomposites with higher properties. The introduction of HNTs into the EPDM/NBR matrix effectively governed the cure behavior of rubber blend, also improved the thermal, mechanical, and crosslinking of rubber blends because of interfacial interaction improvement in the presence of MAH-*g*-EPDM compatibilizer. The mechanical properties analysis proved that the introduction of HNTs into the EPDM/NBR matrix leads to a higher tensile strength and modulus of the nanocomposites by about 45% and 100%, respectively. However, there was a decrease in elongation at break with higher concentrations of nanotubes. Theoretical prediction of stiffness of the nanocomposites suggested a good agreement between the theoretical modulus and experimental values, but some obvious deviation is observed at low loading levels, possibly because of the dominance of interaction contribution to modulus in such a complex system, which could not be detected by the model. DMTA measurements revealed a higher storage modulus for the nanocomposites with higher HNTs loading. However, there is some reduction in damping factor with the introduction of nanotubes into the rubber matrix. The results of swelling analysis of the nanocomposites unraveled a lower solvent uptake with higher amount of HNTs. Thermogravimetric analysis (TGA) of EPDM/NBR/HNTs nanocomposites indicated that the introduction of nanotubes into the rubber matrix leads to a higher thermal stability, particularly at higher temperatures (above 500 °C), where HNTs resists against thermal degradation.

**Author contribution** SMRP Writing original draft, Supervision; GN Methodology; MM Sample preparation and analysis; MHRG Formal analysis; MW Investigation; AE Review and editing; OA Formal analysis; MRS Supervision, Conceptualization, Review and editing—last version.

## Declarations

**Conflict of interest** Authors declare no conflicts of interest.

**Open Access** This article is licensed under a Creative Commons Attribution 4.0 International License, which permits use, sharing, adaptation, distribution and reproduction in any medium or format, as long as you give appropriate credit to the original author(s) and the source, provide a link to the Creative Commons licence, and indicate if changes were made. The images or other third party material in this article are included in the article's Creative Commons licence, unless indicated otherwise in a credit line to the material. If material is not included in the article's Creative Commons licence and your intended use is not permitted by statutory regulation or exceeds the permitted use, you will need to obtain permission directly from the copyright holder. To view a copy of this licence, visit <http://creativecommons.org/licenses/by/4.0/>.

## References

1. Khosravi A, Fereidoon A, Khorasani MM, Saeb MR (2022) Experimental and theoretical mechanical behavior of compatibilized polylactic acid/polyolefin elastomer blends for potential packaging applications. *Iran Polym J* 31:1–13
2. Mishra V (2021) Effect of carbon black and graphene on the performance of EPDM rubber composites: a short review. *IOP Conf Ser Mater Sci Eng* 1116(1):012004
3. Botros S, Tawfic M (2005) Compatibility and thermal stability of EPDM-NBR elastomer blends. *J Elastomers Plast* 37(4):299–317
4. Botros S, Tawfic M (2006) Synthesis and characteristics of MAH-g-EPDM compatibilized EPDM/NBR rubber blends. *J Elastomers Plast* 38(4):349–365
5. Manoj K, Kumari P, Unnikrishnan G (2011) Cure characteristics, swelling behaviors, and mechanical properties of carbon black filler reinforced EPDM/NBR blend system. *J Appl Polym Sci* 120(5):2654–2662
6. Basha SKT, Divya R, Menon AU, Ashok N, Balachandran M (2018) Cure and degradation kinetics of sulfur cured nanocomposites of EPDM-NBR rubber blends. *Mater Today Proc* 5(11):23586–23595
7. Hoikkanen M, Poikelispää M, Das A, Honkanen M, Dierkes W, Vuorinen J (2015) Effect of multi-walled carbon nanotubes on the properties of EPDM/NBR dissimilar elastomer blends. *Polym Plast Technol Eng* 54(4):402–410
8. Ghassemieh E (2009) Enhancement of the properties of EPDM/NBR elastomers using nanoclay for seal applications. *Polym Compos* 30(11):1657–1667
9. Ersali M, Fazeli N, Naderi G (2012) Preparation and properties of EPDM/NBR/organoclay nanocomposites. *Int Polym Proc* 27(2):187–195
10. Jovanović V, Samaržija-Jovanović S, Budinski-Simendić J, Marković G, Marinović-Cincović M (2013) Composites based on carbon black reinforced NBR/EPDM rubber blends. *Compos B Eng* 45(1):333–340
11. Paran SMR, Naderi G, Javadi F, Shemshadi R, Saeb MR (2020) Experimental and theoretical analyses on mechanical properties and stiffness of hybrid graphene/graphene oxide reinforced EPDM/NBR nanocomposites. *Mater Today Commun* 22:100763
12. Vahabi H et al (2018) Short-lasting fire in partially and completely cured epoxy coatings containing expandable graphite and halloysite nanotube additives. *Prog Org Coat* 123:160–167
13. Kamble R, Ghag M, Gaikawad S, Panda BK (2012) Halloysite nanotubes and applications: a review. *J Adv Sci Res* 3(2):25–29
14. Du M, Guo B, Jia D (2010) Newly emerging applications of halloysite nanotubes: a review. *Polym Int* 59(5):574–582
15. Krishnaiah P et al (2021) Mechanical, thermal and dynamic-mechanical studies of functionalized halloysite nanotubes reinforced polypropylene composites. *Polym Polym Compos* 29(8):1212–1221
16. Paran SR, Naderi G, Ghoreishy MR (2016) Effect of halloysite nanotube on microstructure, rheological and mechanical properties of dynamically vulcanized PA6/NBR thermoplastic vulcanizates. *Soft Mater* 14(3):127–139



17. Kadlec P, Polanský R (2018) Effect of different type of polyethylene matrix on the properties of PE/HNT composites. In: 2018 IEEE 2nd international conference on dielectrics (ICD). IEEE, pp 1–4
18. Rooj S, Das A, Thakur V, Mahaling R, Bhowmick AK, Heinrich G (2010) Preparation and properties of natural nanocomposites based on natural rubber and naturally occurring halloysite nanotubes. *Mater Des* 31(4):2151–2156
19. Pasbakhsh P, Ismail H, Fauzi MA, Bakar AA (2010) EPDM/modified halloysite nanocomposites. *Appl Clay Sci* 48(3):405–413
20. Vahabi H, Saeb MR, Formela K, Cuesta J-ML (2018) Flame retardant epoxy/halloysite nanotubes nanocomposite coatings: exploring low-concentration threshold for flammability compared to expandable graphite as superior fire retardant. *Prog Org Coat* 119:8–14
21. Rawtani D, Agrawal Y (2012) Multifarious applications of halloysite nanotubes: a review. *Rev Adv Mater Sci* 30(3):282–295
22. Kolařík J (1997) Three-dimensional models for predicting the modulus and yield strength of polymer blends, foams, and particulate composites. *Polym Compos* 18(4):433–441
23. Zhou Z, Sarafbidabad M, Zare Y, Rhee KY (2018) Prediction of storage modulus in solid-like poly (lactic acid)/poly (ethylene oxide)/carbon nanotubes nanocomposites assuming the contributions of nanoparticles and interphase regions in the networks. *J Mech Behav Biomed Mater* 86:368–374
24. Zare Y, Rhee KY (2020) Tensile modulus prediction of carbon nanotubes-reinforced nanocomposites by a combined model for dispersion and networking of nanoparticles. *J Market Res* 9(1):22–32
25. Berahman R, Raiati M, Mazidi MM, Paran SMR (2016) Preparation and characterization of vulcanized silicone rubber/halloysite nanotube nanocomposites: Effect of matrix hardness and HNT content. *Mater Des* 104:333–345
26. Akbari V et al (2019) Surface chemistry of halloysite nanotubes controls the curability of low filled epoxy nanocomposites. *Prog Org Coat* 135:555–564
27. Guo B, Lei Y, Chen F, Liu X, Du M, Jia D (2008) Styrene-butadiene rubber/halloysite nanotubes nanocomposites modified by methacrylic acid. *Appl Surf Sci* 255(5):2715–2722
28. Ismail H, Salleh SZ, Ahmad Z (2013) Properties of halloysite nanotubes-filled natural rubber prepared using different mixing methods. *Mater Des* 50:790–797. <https://doi.org/10.1016/j.matdes.2013.03.038>
29. Paran SMR et al (2017) To what extent can hyperelastic models make sense the effect of clay surface treatment on the mechanical properties of elastomeric nanocomposites? *Macromol Mater Eng* 302(7):1700036
30. Paran S, Naderi G, Ghoreishy M, Dubois C (2018) Essential work of fracture and failure mechanisms in dynamically vulcanized thermoplastic elastomer nanocomposites based on PA6/NBR/XNBR-grafted HNTs. *Eng Fract Mech* 200:251–262
31. Zhong B, Jia Z, Hu D, Luo Y, Guo B, Jia D (2016) Surface modification of halloysite nanotubes by vulcanization accelerator and properties of styrene-butadiene rubber nanocomposites with modified halloysite nanotubes. *Appl Surf Sci* 366:193–201. <https://doi.org/10.1016/j.apsusc.2016.01.084>
32. Chopra S, Deshmukh KA, Peshwe D (2017) Theoretical prediction of interfacial properties of PBT/CNT nanocomposites and its experimental evaluation. *Mech Mater* 109:11–17
33. Paran S, Naderi G, Ghoreishy M, Dubois C (2018) Multiscale modeling of polymer systems comprising nanotube-like inclusions by considering interfacial debonding under plastic deformations. *Compos Struct* 194:302–315
34. Paran S, Naderi G, Ghoreishy M (2016) Mechanical properties development of high-ACN nitrile-butadiene rubber/organoclay nanocomposites. *Plast Rubber Compos* 45(9):389–397
35. Paran SMR, Naderi G, Mosallanezhad H, Movahedifar E, Formela K, Saeb MR (2020) Microstructure and mechanical properties of carboxylated nitrile butadiene rubber/epoxy/XNBR-grafted halloysite nanotubes nanocomposites. *Polymers* 12(5):1192
36. Chonkaew W, Minghvanish W, Kunglian U, Rochanawipart N, Brostow W (2011) Vulcanization characteristics and dynamic mechanical behavior of natural rubber reinforced with silane modified silica. *J Nanosci Nanotechnol* 11(3):2018–2024
37. Xiong X, Wang J, Jia H, Fang E, Ding L (2013) Structure, thermal conductivity, and thermal stability of bromobutyl rubber nanocomposites with ionic liquid modified graphene oxide. *Polym Degrad Stab* 98(11):2208–2214

## Authors and Affiliations

Seyed Mohamad Reza Paran<sup>1</sup> · Ghasem Naderi<sup>1</sup> · Moslem Mirzaee<sup>1</sup> ·  
Mir Hamid Reza Ghoreishy<sup>1</sup> · Marcin Włoch<sup>2</sup> · Amin Esmaeili<sup>3</sup> · Otman Abida<sup>4</sup> ·  
Mohammad Reza Saeb<sup>2</sup> 

<sup>1</sup> Department of Polymer Processing, Iran Polymer and Petrochemical Institute, P.O. Box 14965/115, Tehran, Iran

<sup>2</sup> Department of Polymer Technology, Faculty of Chemistry, Gdańsk University of Technology, G. Narutowicza 11/12, 80-233 Gdańsk, Poland

<sup>3</sup> Department of Chemical Engineering, School of Engineering Technology and Industrial Trades, University of Doha for Science and Technology (UDST), 24449 Arab League St, Doha, Qatar

<sup>4</sup> African Sustainable Agriculture Research Institute (ASARI), Mohammed VI Polytechnic University (UM6P), Laâyoune 70000, Morocco